Appl Phys B (2009) 97: 835–840
DOI 10.1007/s00340-009-3770-y

Applied Physics B
Lasers and Optics

An optical study of vacuum evaporated amorphous $Ge_{20}Te_{80-x}Bi_x$ thin films using transmission and reflection spectra

A. Sharma · P.B. Barman

Received: 30 March 2009 / Revised version: 17 August 2009 / Published online: 18 October 2009

Abstract The present paper reports the effect of Bi addition on the optical behavior (optical band gap and refractive index) of $Ge_{20}Te_{80-x}Bi_x$ (where $x = 0$, 1.5, 2.5, 5.0) glassy alloys by analyzing the transmission and reflection spectra of their thin films in the 900–2400 nm range. Films are deposited on glass substrate using a thermal evaporation technique under vacuum. Various optical parameters viz. refractive index, extinction coefficient, absorption coefficient, optical band gap, etc. are determined and the effect of Bi incorporation on these parameters is studied. The refractive index has been found to increase with increasing Bi content over the entire spectral range and this behavior is due to the increased polarizability of the larger Bi atomic radius (1.46 Å) compared to Te atomic radius (1.36 Å). Dispersion energy, E_d, average energy gap, E_0 and static refractive index, n_0 is calculated using Wemple–DiDomenico model. Optical band gap is estimated using Tauc's extrapolation and is found to decrease from 0.86 to 0.73 eV with the Bi addition. This behavior of the optical band gap is interpreted in terms of the electronegativity difference of the atoms involved and the cohesive energy of the system.

PACS 78.55.Qr · 77.84.Bw · 78.20.Ci

1 Introduction

There are numerous applications in science and technology areas for optical coatings, such as communication, sensing, imaging and display. It is essential to know the different parameters of the coating materials, such as refractive indices, absorption coefficients and optical band gap, while designing and manufacturing the optical coatings and devices. Chalcogenide glasses have attracted the attention of many investigators due to their potential applications in IR optics, photonics device, reversible optical recording, memory switching, inorganic photo resists, antireflection coating, optical data storage, frequency doubling, optical limiter etc. [1–8]. Due to their high refractive index (ranging between 2.0 and 3.5) and optical band gap lying in the sub-band gap region, chalcogenide glasses are used as core materials for optical fibers which are further used for transmission, especially when short length and flexibility is required [9–11]. One of the most advantageous characteristics of these materials is in phase change optical memory technology. Phase change recording materials are designed to have at least two structural forms, amorphous and crystalline, which can coexist at room temperature. Phase change applications utilize differences in optical and electrical properties between the amorphous and crystalline phases of the same material. Optical storage applications utilize small differences (approximately 20%) in the reflectivity [12], while electronic applications utilize a large difference (a factor of approximately 10^3) in electrical conductivity [13]. These materials can be optically switched between the amorphous and crystalline states by the energy contained in a laser beam. Infrared optical fibers operating at the 2–12 μm wavelength region are required for infrared sensing applications such as radiometric thermometry, and CO_2 laser power applications such as laser surgery [14]. The Te based chalcogenide glasses are used for such applications because their infrared absorption edges are located in a wavelength region above 12 μm [15]. However, only a few compositions such as Ge–Te and As–Te based glasses have been investigated as mem-

A. Sharma (✉) · P.B. Barman
Department of Physics, Jaypee University of Information Technology, Waknaghat, Solan, H.P. 173215, India
e-mail: ambikasharma2004@yahoo.co.in
Fax: +91-179-2245362

ory switching glasses [16–20]. Impurity effects in chalcogenide glasses have importance in the fabrication of glassy semiconductors. These impurity atoms are supposed to satisfy all the valence requirements when they enter the glassy network and therefore are not supposed to play the role of acceptors or donors. The effect of impurity atoms in chalcogenide glasses depends upon the composition of the glasses, chemical nature of impurity, and the value of impurity concentration. Several authors [21–23] have reported the impurity effects in various chalcogenide glasses. We have chosen $Ge_{20}Te_{80}$ as base composition, which is just at the stiffness threshold with coordination number 2.4 and Bi as dopant. The composition $Ge_{20}Te_{80-x}Bi_x$ can be taken as phase separated glasses, with glassy Bi_2Te_3 clusters embedded in the background matrix of $GeTe_2$ and Te chains or layers. As Bi concentration is increased in the binary alloy $Ge_{20}Te_{80}$, the Bi_2Te_3 clusters, having tetradymite structure find themselves in a matrix of increased mechanical rigidity. These types of structural changes have a numerous effects on the optical parameters like the refractive index and optical band gap.

An increasing concentration of Bi in Ge–Te glassy alloy is responsible for the band tailing and broadening of the valence band, which is further known to reduce the width of optical band gap. The aim of the present investigation is to study the effect of Bi incorporation on the optical properties of Ge–Te matrix. Various optical parameters are determined by using the transmission and reflection spectra of $Ge_{20}Te_{80-x}Bi_x$ chalcogenide thin films.

2 Experimental details

Glassy alloys of the $Ge_{20}Te_{80-x}Bi_x$ ($x = 0$, 1.5, 2.5, 5.0) system were prepared by the melt quenching technique. Materials (99.999% purity) were weighed (4 g for each batch using a Mettler Toledo PL83-S) according to their atomic weight percentage and sealed in evacuated (10^{-4} Pa) quartz ampules. The sealed ampules were kept inside a furnace where the temperature was increased up to 1200°C at a heating rate of 3–4°C min^{-1}. The ampules were frequently rocked for 12 h at the highest temperature to make the melt homogeneous. The quenching was done in ice cold water. Films of bulk glasses were deposited on microscopic glass substrates using the vacuum evaporation technique at a base pressure of 10^{-4} Pa (Hindhivac Model No. 12A4D). The thickness of the solid films has been monitored during depositions by using a thickness monitor (DTM-101) (with an uncertainty of ±20 nm). The compositions of the evaporated samples have been measured by an electron microprobe analyzer (JEOL 8600 MX) on different spots (size ≈2 μm). For the composition analysis, the constitutional elements (Ge, Te and Bi) and the bulk original alloys, i.e. $Ge_{20}Te_{80-x}Bi_x$ are taken as reference samples. The composition of 2×2 cm^2 sample is uniform within the measurement accuracy of about ±1.5–2.0%. The bulk as well as the thin films of the samples prepared were characterized by the X-ray diffraction (XRD) technique (Rigaku Geiger Flex 3KW Diffractometer, Cu Kα source). No prominent peak has been observed in the spectra, indicating the amorphous nature of both the bulk and thin films. The normal incidence transmittance and reflectance spectra in the spectral range 700–2400 nm of films were obtained by a double beam ultraviolet–visible–near infrared spectrophotometer (Perkin Elmer Lambda-750). All measurements were performed at room temperature (300 K).

3 Results and discussion

3.1 Behavior of refractive index: WDD model

The transmission and reflection spectra of the thin film samples under study are plotted in Fig. 1. It is clear from Fig. 1 that a red shift occurs in the interference free region with the Bi addition. Such a shift in the spectrum of the composition studied is a consequence of compositional dependence of the optical band gap and it also gives an enhanced value of the refractive index. The optical absorption coefficient (α) is one of the important parameters and strongly depends upon the transmittance (T) and reflectance (R). α is evaluated by using the relation [24]

$$\alpha = \frac{2.303}{d} \log\left(\frac{1-R}{T}\right), \tag{1}$$

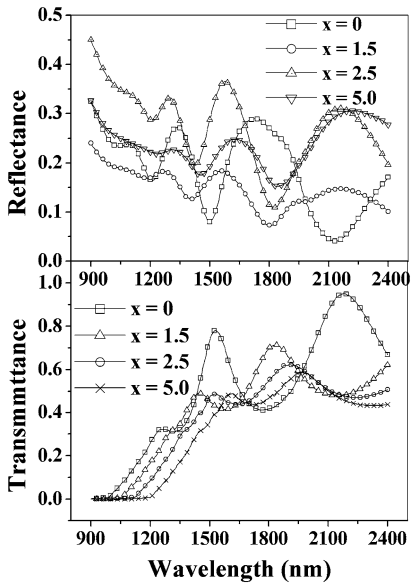

Fig. 1 (**a–b**) Plot of transmission and reflection versus wavelength (nm) for $Ge_{20}Te_{80-x}Bi_x$ thin films

Table 1 Values of coordination number (m), refractive index (n), extinction coefficient (k), dielectric constant (ε_r), dielectric loss (ε_i) and optical conductivity (σ) are given at 1100 nm and static refractive index (n_0), for $Ge_{20}Te_{80-x}Bi_x$ thin films

x	m	n	k	ε_r	ε_i	$\sigma \times 10^{12}(s^{-1})$	n_0	ε_∞
0	2.4	2.88	0.0031	8.29	0.018	2.42	2.27	5.15
1.5	2.415	3.06	0.0046	9.36	0.028	3.87	2.40	5.76
2.5	2.425	3.31	0.0070	10.96	0.046	7.04	2.56	6.55
5.0	2.45	3.49	0.01051	12.18	0.070	10.25	3.06	9.33

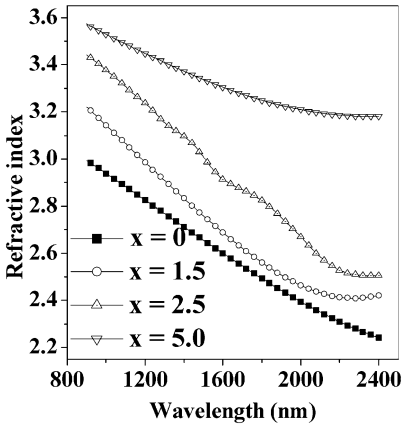

Fig. 2 Plot of refractive index (n) versus wavelength (nm) for $Ge_{20}Te_{80-x}Bi_x$ thin films

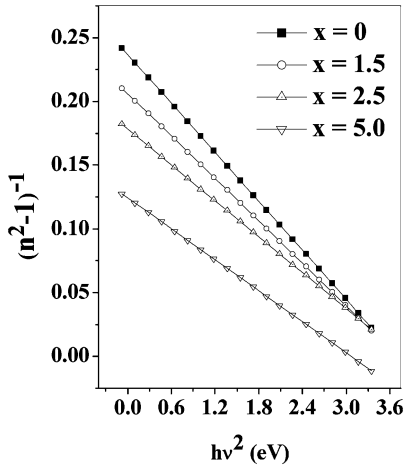

Fig. 3 Plot of $(n^2-1)^{-1}$ versus $(h\nu)^2$ for $Ge_{20}Te_{80-x}Bi_x$ thin films

where d is the film thickness ($d \approx 500$ nm for all the samples with an uncertainty of ± 20 nm). α has been found to be of the order of 10^4 cm^{-1}. For air as first medium with refractive index $= 1$ and considering the film as second medium, which is highly absorbing in nature, the refractive index (n) has been calculated using the relation [24]

$$R = \frac{(n-1)^2 + k^2}{(n+1)^2 + k^2} \tag{2}$$

where k is the extinction coefficient and has been calculated using $k = \lambda\alpha/4\pi$ [24]. It has been observed that both n and k decreases with increasing wavelength, which further indicates the normal dispersion behavior of the films under study.

It is also evident from Fig. 2 that with the increase of Bi content n increases. High refractive index values are beneficial for most of the technological applications as they lead to compact circuit designs. This increase in n is related to the increased polarizability of the larger Bi atomic radius (1.46 Å) compared to the Te atomic radius (1.36 Å). The larger the atomic radius of the atom, the larger will be its polarizability and consequently according to the Lorentz-Lorenz relation [25] the larger will be refractive index. Since in our system the less polarized atom Te is replaced by the more polarized atom Bi, the refractive index of the system increases. The results are also justified with a clear red shift observed in the optical absorption edge as shown in Fig. 1.

The calculated value of n, k and α for thin films under study typically at 1100 nm is shown in Table 1.

The spectral dependence of the refractive index has been analyzed in terms of the Wemple-DiDomenico (WDD) model [26], which assumes that the properties of $Ge_{20}Te_{80-x}Bi_x$ thin films at high frequency could be treated as a single oscillator having the expression

$$n^2 - 1 = \frac{E_d E_0}{E_0^2 - (h\nu)^2}, \tag{3}$$

where $h\nu$ is the photon energy, E_0 is the single oscillator energy (also called average energy gap) and E_d is the dispersion energy, which is a measure of average strength of the interband optical transitions. The oscillator parameters are determined by plotting refractive index factor $(n^2-1)^{-1}$ versus $(h\nu)^2$ and by fitting a straight line to the points as shown in Fig. 3. In Fig. 3, slope $= (E_0E_d)^{-1}$ and the intercept on the vertical axis $= (E_0/E_d)$. The value of E_d and E_0 are calculated using these two relations and are listed in Table 2. The parameter E_d is related to other the physical parameters by the simple empirical relation proposed by the WDD model, i.e. $E_d = \beta N_c Z_a N_e$, where β is a two valued constant with either an ionic or a covalent value ($\beta = 0.26 \pm 0.03$ eV for ionic materials and $\beta = 0.37 \pm 0.04$ eV for covalent materials), N_c is the effective coordination number of the cation nearest neighbor to the anion, Z_a is the formal chemical valance of the anion and

Table 2 Excess Te–Te bonds, cohesive energy (CE), dispersion energy (E_d), oscillator energy (E_0),optical band gap (E_g) and $B^{1/2}$ for $Ge_{20}Te_{80-x}Bi_x$ thin films

x	Excess Te–Te bonds	CE(eV)	E_d(eV)	E_0(eV)	E_g(eV)	$B^{1/2}$
0	80.0	2.26	7.48	1.80	0.86	400
1.5	72.5	2.21	8.22	1.73	0.83	321.54
2.5	67.5	2.18	9.46	1.70	0.78	195.7
5.0	55.0	2.10	12.5	1.50	0.73	83.68

N_e is the effective number of valence electrons per anion. The increase in the observed value of E_d with Bi content is only due to the increase in the value of N_c, which is calculated by using the relation $N_c = 0.01(aN_{\mathrm{Ge}} + bN_{\mathrm{Te}} + cN_{\mathrm{Bi}})$, where N_{Ge}, N_{Te} and N_{Bi} are the coordination numbers for Ge, Te and Bi and a, b, c are their at.% respectively. The value of N_c for the system under investigation is found to increase from 2.40 to 2.45 as shown in Table 1.

The single oscillator energy E_0, also known as the WDD gap, corresponds to the distance between the centers of gravity of the valence and conduction band. It is therefore related to the bond energy of different chemical bonds present in the system. Moreover E_0 can also be used to estimate an approximate value of the optical energy gap (E_g) by using an empirical relation proposed by Tanaka [27], i.e. $E_o \approx 2 \times E_g$. It is clear from Table 2 that the values obtained by using the above relation are in good agreement with that obtained by using Tauc's extrapolation method. Similar results have also been reported earlier by various other researchers [28, 29].

The value of the static refractive index n_0, has been calculated by extrapolating $h\nu$ to zero in Fig. 3, and (3) reduces to

$$n_0 = (1 + E_d/E_0)^{1/2}. \tag{4}$$

The calculated values of n_0, for films under investigation are found to increase with Bi content. The high frequency dielectric constants (ε_∞) have been calculated from the relation $\varepsilon_\infty = (n_0)^2$ and are reported in Table 1. The dielectric constant (ε_r) and dielectric loss (ε_i) have been determined from the relation $\varepsilon_r = n^2 - k^2$ and $\varepsilon_i = 2nk$ for $Ge_{20}Te_{80-x}Bi_x$ thin films. The optical conductivity is calculated from the equation $\sigma = \alpha nc/4\pi$, where c is the velocity of light. The optical conductivity has been found to increase with increasing Bi content. This increase may be a consequence of an increased density of localized states in the gap itself due to the appearance of new defect states and Bi containing structural elements [30]. The dielectric constant, dielectric loss and optical conductivity directly depend on n, k and α and hence follow similar trends. The values of $\varepsilon_r, \varepsilon_i$, and σ are given in Table 1 at 1100 nm.

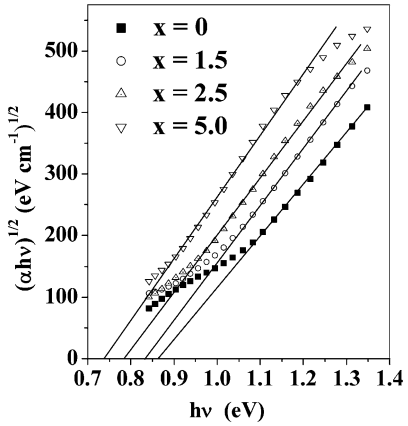

Fig. 4 Plot of $(\alpha h\nu)^{1/2}$ versus $h\nu$ for $Ge_{20}Te_{80-x}Bi_x$ thin films

3.2 Optical band gap determination

The optical band gap (E_g) has been determined according to the generally accepted 'non direct transition' model for amorphous semiconductors proposed by Tauc [31], which assumes that the densities of electron states in the valence and conduction bands, near the band gap, have a parabolic distribution. The relation is

$$\alpha h\nu = B(h\nu - E_g)^2 \tag{5}$$

where $B^{1/2}$ is the so called Tauc slope.

The graph between $(\alpha h\nu)^{1/2}$ and $h\nu$ for $Ge_{20}Te_{80-x}Bi_x$ films is shown in Fig. 4. The non-linear nature of the graph provides evidence that the transition in the forbidden gap is of indirect type. It is also evident from the figure that the optical band gap decreases with the addition of Bi content. This decrease in optical band gap may be correlated with the electronegativity difference of the elements involved. According to Kastner et al. [32], the valence band in chalcogenide glasses is constituted by lone pair p-orbitals contributed by the chalcogen atoms. These lone pair electrons will have a higher value of energies adjacent to electropositive atoms than those of electronegative atoms. Therefore the addition of electropositive elements to the alloy may raise the energy of lone pair states, which is further responsible for the broadening of the valence band inside the forbidden gap. The electronegativities of Ge, Te and Bi are 2.01, 2.1 and 2.0 respectively. Since Bi is more electropositive than Te, the substitution of Bi for Te may raise the energy of some lone pair states and hence broaden the valence band. This leads to band tailing and hence shrinking of the band gap. This is also verified by considering the B factor in (5), which is inversely related to the product of static refractive index, n_0, and localized state tail width, ΔE_{tail} [33–35]. It is therefore a clear indicator of the degree of randomness of the atomic structure of amorphous semiconductors. From the value of the Tauc slope $B^{1/2}$ (Table 2) it is clear that ΔE_{tail} increases

with increasing Bi content since $\Delta E_{\text{tail}} \propto [n_0 B]^{-1}$. It may be mentioned here that the decrease found in the values of parameter B is much more pronounced than the increase observed in the values of n_0. The value of band gap decreases from 0.86 to 0.73 eV as the Bi content is increased from 0 to 5 at.% in the Ge–Te glassy alloy (Table 2). The optical band gap is a bond sensitive property [36]. Thus a decrease in optical band gap may also be explained on the basis of the average bond energy or cohesive energy of the system. The cohesive energy (CE), defined as the stabilization energy of an infinitely large cluster of the material per atom is determined by summing the bond energies of the consequent bonds expected in the material. This behavior is equivalent to assuming a simplified model consisting of non-interacting electron pair bonds highly localized between adjacent pair of atoms. The cohesive energy (CE) of the prepared bulk samples is evaluated using the relation [37]

$$CE = \sum (C_i D_i / 100) \tag{6}$$

where C_i and D_i are the number of expected chemical bonds and energy of each bond respectively. The bond energy of heteropolar bonds is calculated by using the Pauling method [38]. According to the chemical bond approach (CBA) [39], atoms combine more favorably with atoms of a different kind rather than with atoms of the same kind and bonds are formed in the sequence of decreasing bond energies until all the available valences are satisfied. Consequently bonds between like atoms will only occur if there is an excess of certain type of atoms. In the above-mentioned system, Bi enters into the Ge–Te system and saturates the Bi–Te bonds, thus decreasing the concentration of Ge–Te bonds. Since the bond energy of Bi–Te bond (125.6 kJ/mol) is lower than that of the Ge–Te bond (156.7 kJ/mol), the average bond energy and hence CE of the system decreases. The excess Te–Te bonds and CE of the system are calculated and tabulated in Table 2.

4 Conclusion

The transmission and reflection spectra of vacuum evaporated $Ge_{20}Te_{80-x}Bi_x$ thin films taken at normal incidence have been analyzed in the spectral range 900–2400 nm and the various optical parameters are calculated. The results indicate that n increases with the increasing Bi content, which is related to the increased polarizability of the larger Bi atom compared to Te. The dispersion parameters E_d, E_0 and n_0 are discussed in terms of the WDD model. It has been observed that E_d and n_0 increases, while E_0 decreases with increase in Bi content. The optical absorption in the given system seems to be of non-direct type and the optical band gap determined in the strong absorption region by Tauc's extrapolation is found to decrease from 0.86 to 0.74 eV with the addition of Bi content. The decrease in average bond energy and hence optical band gap is interpreted in terms of the cohesive energy and electronegativity difference of the atoms involved.

References

1. M. Frumar, T. Wagner, Curr. Opin. Solid State Mater. Sci. **7**, 117 (2003)
2. A. Znobrik, J. Stetzif, I. Kavich, V. Kavich, V. Osipenko, I. Zachko, N. Balota, O. Jakivchuk, Ukr. Phys. J. **26**, 212 (1981)
3. J.S. Sanghera, I.D. Aggarwal, J. Non-Cryst. Solids **656–657**, 6 (1999)
4. K. Schwartz, *The Physics of Optical Recording* (Springer, Berlin, 1993)
5. A. Bradley, *Optical Storage for Computers Technology and Applications* (Ellis Harwood, New York, 1989)
6. J. Bradangna, S.A. Keneman, in *Holographic Recording Media*, ed. by H.M. Smith (Springer, Berlin, 1977)
7. P.A. Thielen, L.B. Shaw, J.S. Sanghera, I.D. Aggarwal, Opt. Express **11**, 3228 (2003)
8. J. Troles, F. Smektala, G. Boudebsa, A. Monteila, B. Bureau, J. Lucas, J. Optoelectron. Adv. Mater. **4**, 729 (2002)
9. A. Elshafie, A.A. Abdel, Physica B **269**, 69 (1999)
10. K. Abe, H. Takebe, K. Maronaga, J. Non-Cryst. Solids **212**, 143 (1997)
11. K. Wei, D.P. Machewirth, J. Wenzel, G.H. Sigel, J. Non-Cryst. Solids **182**, 257 (1995)
12. S. Hudgens, B. Johnson, MRS Bull. **29**, 829 (2004)
13. J.D. Maimon, K.K. Hunt, L. Burcin, J. Rodgers, IEEE Trans. Nucl. Sci. **50**, 1878 (2003)
14. T. Katsuyama, H. Matsumura, *Infrared Optical Fibers* (Adam Hilgers, London, 1989). p. 212
15. T. Katsuyama, H. Matsumura, Appl. Phys. Lett. **49**, 22 (1986)
16. T. Takamori, R. Roy, G.J. Mccarthy, Mater. Res. Bull. **5**, 529 (1970)
17. S. Lizima, M. Suzi, M. Kikuchi, K. Tanaka, Solid State Commun. **8**, 153 (1970)
18. J.A. Savaga, J. Mater. Sci. **6**, 964 (1971)
19. J.A. Savaga, J. Non Cryst. Solids **11**, 121 (1972)
20. S. Bordas, V.J. Casas, N. Clavaguera, M.T. Clavaguera Mora, Thermochim. Acta **28**, 387 (1973)
21. M.A. Majeed Khan, M. Zulfequar, M. Hussain, J. Phys. Chem. Solids **62**, 1093 (2001)
22. I. Sharma, S.K. Tripathi, P.B. Barman, J. Phys. D, Appl. Phys. **40**, 4460 (2007)
23. E.R. Shaaban, M.A. Kaid, S.E. Moustafa, A. Adel, J. Phys. D, Appl. Phys **41**, 125301 (2008)
24. M.M. El-Raheem Abd, J. Phys., Condens. Matter. **19**, 216209 (2007)
25. S.R. Elliott, *The Physics and Chemistry of Solids* (Wiley, Chichester, 2000)
26. S.H. Wemple, M. DiDomenico, Phys. Rev. B **3**, 1338 (1971)
27. K. Tanaka, Thin Solid Films **66**, 271 (1980)
28. J.M. Gonzalez-Leal, A. Ledesma, A.M. Bernal-Oliva, R. Prieto-Alcon, E. Marquez, J.A. Angel, J. Carabe, Mater. Lett. **39**, 232 (1999)
29. T.I. Kosa, T. Wagner, P.J.S. Ewen, A.E. Owen, Philos. Mag. B **311**, 71 (1995)
30. N.F. Mott, E.A. Davis, Philos Mag. **22**, 903 (1970)
31. J. Tauc, *Amorphous and Liquid Semiconductors* (Plenum, New York, 1979)
32. M. Kastner, D. Adler, H. Fritzsche, Phys. Rev. Lett. **37**, 1504 (1976)

33. N.F. Mott, E.A. Davis, *Electronic Processes in Non-Crystalline Materials*, 2nd edn. (Clarendon, Oxford, 1979)
34. A.R. Zanatta, I. Chambouleyron, Phys. Rev. B **53**, 3833 (1996)
35. L. Tichý, H. Tichá, P. Nagels, R. Callaerts, Mater. Lett. **36**, 294 (1998)
36. A.K. Pattanaik, A.J. Srinivasan, Optoelectron Adv. Mater. **5**, 1161 (2003)
37. S.A. Fayek, M.R. Balboul, K.H. Marzouk, Thin Solid Films **515**, 7281 (2007)
38. L. Pauling, in *Die Nature der Chemischen Bindung* (VCH, Weinheim, 1976), pp. 80–89
39. J. Biecerano, S.R. Ovshinesky, J. Non-Cryst. Solids **74**, 75 (1985)